Soft Matter

Accepted Manuscript

ROYAL SOCIETY OF CHEMISTRY

www.rsc.org/softmatter

Cite this: DOI: 10.1039/c0xx00000x

www.rsc.org/xxxxxx

ARTICLE TYPE

Aggregation behavior of a gemini surfactant with a tripeptide spacer

Meina Wang, Yuchun Han, Fulin Qiao and Yilin Wang*

Received (in XXX, XXX) Xth XXXXXXXXX 20XX, Accepted Xth XXXXXXXXX 20XX
DOI: 10.1039/b000000x

A peptide gemini surfactant 12-G(NH_2)LG(NH_2)-12 has been constructed with two dodecyl chains separately attached to the two terminals of a glutamic acid-lysine-glutamic acid peptide and the aggregation behavior of the surfactant was studied in aqueous solution. The 12-G(NH_2)LG(NH_2)-12 molecules form fiber-like precipitates around pH 7.0, and the precipitation range is widened with increasing the concentration. At pHs 3.0 and 11.0, 12-G(NH_2)LG(NH_2)-12 forms soluble aggregates because each molecule carries two positively charged amino groups at the two ends of the peptide spacer at pH 3.0, while each molecule carries one negatively charged carboxyl group in the middle of the peptide spacer at pH 11.0. 12-G(NH_2)LG(NH_2)-12 displays a similar concentration dependent process at these two pHs: forming small micelles above critical micelle concentration and transferring to fibers at pH 3.0 or twisted ribbons at pH 11.0 above the second critical concentration. The fibers formed at pH 3.0 tend to aggregate into bundles with twisted structure. Both the twisted fibers at pH 3.0 and the twisted ribbons at pH 11.0 contain β-sheet structure formed by the peptide spacer.

Introduction

Surfactants have been widely applied in industry and daily life. To reduce the load which surfactants place on the environment, the key solution is to develop efficient but biodegradable, biocompatible and low-toxic surfactants. Peptide surfactants satisfy these needs.[1-3] Moreover, peptide surfactants have low critical micelle concentration, desirable surface activities, mildness features to skin, and excellent antimicrobial activity.[4-8] Therefore, the rapidly growing applications for peptide surfactants can be envisioned, especially in personal care and home care products and pharmaceutical and food formulations.

Numerous peptide surfactants have been synthesized and their physicochemical properties and aggregation behavior were studied.[2,3,9,10] Analogous to traditional surfactants, peptide surfactants are amphiphilic in nature bearing a hydrophilic peptide sequence attached to one or more alkyl chains. The presence of peptide unit in surfactant molecules brings about superior physicochemical properties, unique aggregation behavior and chemical design versatility. Peptide surfactants can self-assemble into micelles, vesicles and a wide array of high-aspect-ratio nanostructures, such as nanofibers, nanotapes, helical ribbons and tubules, with specific biological applications.[11-20] These attractive features of peptide surfactants are inherently related to hydrogen bonding between peptide sequences and hydrophobic interaction between alkyl chains. Therefore, variations in these factors can dramatically affect the aggregation behavior of peptide surfactants. In general, the variations can be realized by modifying surfactant molecular structure or triggered by environmental conditions, such as pH,[11,12] concentration,[6] temperature[21] and so on.[14] Stupp's group[22] synthesized a series of peptide monomeric amphiphiles with valine-glutamic acid dimeric repeats as headgroups and found that the lateral growth of belt-like flat assemblies could be effectively controlled by tuning the number of the repeats. Bianco-Peled's group[23] reported that increasing an alkyl chain length conjugated to model collagen mimetic peptide gives rise to morphological transformation from close-packed spherical micelles to extended strandlike structure. Our group[6] developed a peptide surfactant (C_{12}-Aβ(11-17)) by introducing a key fragment of amyloid β-peptide to dodecanoic acid through an amide bond. The peptide surfactant generated rodlike fibrils at low concentration and pH 3.0, and packed in parallel and transferred into taplike fibrils through lateral association at high concentration. By increasing pH to 10.0, twisted nanoribbons were formed. Although great endeavors have been devoted to understand how molecular structure and environmental conditions affect the aggregate behavior of peptide surfactants, more systematic works are still needed for further comprehension due to their structural diversity and complicated aggregation process.

Peptide gemini surfactants consisting of two alkyl chains and peptide units have been reported in recent several years. Because peptide gemini surfactants combine the characteristics of both peptide surfactants and gemini surfactants, the investigations on peptide gemini surfactants hold importance in both academic aspect and application purpose. It has been proved that peptide gemini surfactants can promote the recovery of smooth and moisturized hair and skin conditions. On the basis of C_{12}-Aβ(11-17),[6] we constructed a peptide gemini surfactant C_{12}-Aβ(11-17)-C_{12} by adding another alkyl chain to another terminal of Aβ(11-17).[12] The presence of two alkyl chains leads to a relatively low critical surfactant concentration required for self-assembly due to remarkable synergistic effect. Moreover the association of two

alkyl chains changes the conformation of the peptide, and twisted ribbons and lamellae are formed. However this gemini surfactant showed very low solubility in water because of the strong hydrogen bonding between the long peptide structures. So if short peptides are used to construct gemini surfactants, the low solubility problem may be solved. Moreover, short peptides with two or three amino acids do not display folding, and are facile to be synthesized and functionalized. Recently Abe's group[24] investigated the self-assembly of peptide gemini surfactants with glutamic acid and lysine as a spacer group, acylglutamyllysilacylglutamate (m-GLG-m where m = 12, 14, and 16, G = glutamic acid, L= lysine). It was found that in aqueous solution, 12-GLG-12 with three negatively charged carboxyl groups self-assembles into spherical micelles over a wide range of concentration up to 32 wt%, and then changes to micellar cubic phase.

In this work, we designed and investigated a tripeptide gemini surfactant 12-G(NH_2)LG(NH_2)-12 with a glutamic acid-lysine-glutamic acid peptide as the spacer. Different from 12-GLG-12,[24] two uncoupled α carboxyl groups of glutamic acids at the terminal peptide sequence in 12-GLG-12 are replaced by two α amino groups in 12-G(NH_2)LG(NH_2)-12. The molecular structure of 12-G(NH_2)LG(NH_2)-12 is illustrated in Scheme 1. Since one carboxyl group and two amino groups have different pH responses, changing pH causes 12-G(NH_2)LG(NH_2)-12 to carry different number and nature of charges, and influences the formation of hydrogen bonds between the spacers, serving as a switch on the self-assembly of the peptide surfactant. In parallel, increasing the concentration of 12-G(NH_2)LG(NH_2)-12 promotes the hydrophobic interaction between the alkyl chains, and in turn affects its self-assembly. Therefore, the effects of pH and concentration on the surface activity, aggregate structure, phase behavior, intermolecular interaction and the secondary structure have been investigated in the 12-G(NH_2)LG(NH_2)-12 solution.

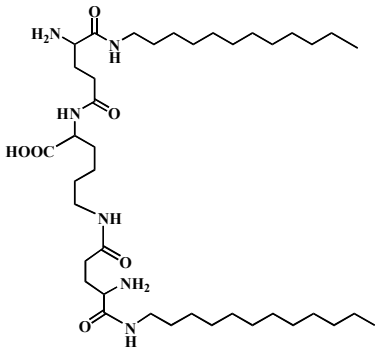

Scheme. 1 Chemical structure of tripeptide gemini surfactant 12-G(NH_2)LG(NH_2)-12.

Experimental section

Materials

The peptide gemini surfactant 12-G(NH_2)LG(NH_2)-12 was designed by us and its synthesis and purification were carried out by GL Biochem (Shanghai) Ltd. The structure of 12-G(NH_2)LG(NH_2)-12 was confirmed by ^{1}H NMR and mass spectra (see Supporting Information), and the purity of 12-G(NH_2)LG(NH_2)-12 was above 99% checked by high-performance liquid chromatography. All of inorganic reagents (> 99.5%) were purchased from Beijing Chemical Co. Milli-Q water (18.2 MΩ·cm) was used throughout.

Potentiometric pH titration

12-G(NH_2)LG(NH_2)-12 was first dissolved in pure water at a concentration of 0.20 mM, and then the solution pH was adjusted to 2.0 with a small volume of 0.10 M HCl standard solution. Then 0.10 M NaOH standard solution was gradually added into this solution in small portions. The pH values were recorded by a pHS-2C acidity meter and the temperature was kept at 25.0 ± 0.1 °C. The electrode was calibrated with a standard buffer solution before being used.

Turbidimetric titration

The turbidity change of the 12-G(NH_2)LG(NH_2)-12 solution at different pHs, reported as 100 - % T, was measured at 450 nm using a Brinkman PC920 probe colorimeter thermostatted at 25.0 ± 0.1 °C. All measured values were corrected by subtracting the turbidity of Milli-Q water.

ζ-Potential measurements

ζ-potential measurements of the 0.20 mM 12-G(NH_2)LG(NH_2)-12 solutions at different pHs were performed with a Malvern Zetasizer Nano-ZS instrument (ZEN3600, Malvern Instruments, Worcestershire, U.K.) equipped with a 4 mW He−Ne laser at a wavelength of 633 nm. Disposable capillary cells (DTS1060C) were used for the measurements. The ζ potentials were calculated from the mobility measured during an electrophoretic light scattering (ELS) experiment using the Hemholtz-Smoluchowski relationship. All experiments were performed at room temperature of around 25 °C.

Surface tension

Surface tension measurements for the 12-G(NH_2)LG(NH_2)-12 solutions at pHs 3.0 and 11.0 were carried out by drop volume method. Each surface tension value (γ) was obtained by averaging at least five consistent measured values. The standard error of surface tension data is 1 mN/m. The measurement was conducted at 25.00 ± 0.05°C using a thermostat.

Isothermal titration microcalorimetry (ITC)

Calorimetric measurements were conducted using a TAM 2277-201 microcalorimetric system (Thermometric AB, Järfälla, Sweden) with a stainless steel sample cell of 1 mL at 25.00 ± 0.01 °C. The cell was initially loaded with water at pHs 3.0 or 11.0, and then concentrated 12-G(NH_2)LG(NH_2)-12 solution at the corresponding pH was injected into the stirred sample cell in portions of 10 μL using a 500μL Hamilton syringe controlled by a Thermomotric 612 Lund pump. The system was stirred at 60 rpm with a gold propeller continuously until the desired range of concentration had been covered. The observed enthalpy (ΔH_{obs}) was obtained by integration over the peak for each injection in the plot of heat flow against time.

Circular dichroism (CD)

The 12-G(NH_2)LG(NH_2)-12 solutions at pHs 3.0 and 11.0 were put in a 0.1 or 1 cm quartz cell and analyzed on a JASCOJ-815 spectrophotometer at room temperature. Scans were obtained in a range from 190 to 260 nm by taking points at 0.5 nm, with an

integration time of 0.5 s. Four spectra were averaged to improve the signal-to-noise ratio and smoothed using the noise reducing option in the software supplied by the vender.

Scanning electron microscopy (SEM)

The morphology of the 0.20 mM 12-G(NH_2)LG(NH_2)-12 solution at pH 7.0 was imaged with a field-emission scanning electron microscope (Hitachi S-4800). The samples were prepared by freezing a small drop of the 12-G(NH_2)LG(NH_2)-12 solution on a clean silica wafer with liquid nitrogen so that the microstructures of the precipitates can be well retained. Immediately afterwards, the frozen samples were lyophilized under vacuum at about -50 °C. Finally, a 1-2 nm Pt coating completed the sample preparation.

Cryogenic transmission electron microscopy (Cryo-TEM)

The 12-G(NH_2)LG(NH_2)-12 solutions at pHs 3.0 and 11.0 were embedded in a thin layer of vitreous ice on freshly carbon-coated holey TEM grids. Then the grids were plunged into liquid ethane cooled by liquid nitrogen. Frozen hydrated specimens were imaged by using an FEI Tecnai 20 electron microscope (LaB6) operated at 200 kV with the low-dose mode (about 2000 e/nm^2) and the nominal magnification of 50000. For each specimen area, the defocus was set to 1-2 μm. Images were recorded on Kodak SO163 films and then digitized by Nikon 9000 with a scanning step 2000 dpi corresponding to 2.54 Å/pixel.[25]

Results and discussion

Charge variations with pH

The charge situation of the 12-G(NH_2)LG(NH_2)-12 molecules depends on the pH condition of solutions, so the variation of pH directly affects the electrostatic interaction and hydrogen bond between the surfactant molecules. Thus, knowledge of the protonation constants (pK_a) of 12-G(NH_2)LG(NH_2)-12 is essential to elucidate the self-assembly in aqueous solution.

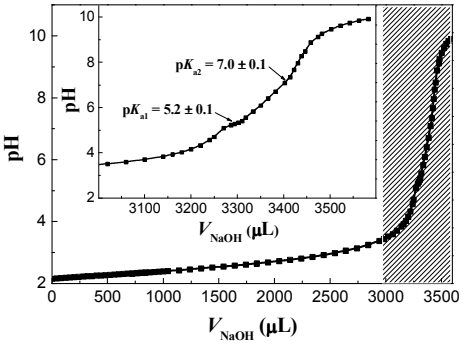

Fig. 1 pH titration curve of 0.20 mM 12-G(NH_2)LG(NH_2)-12 at 25.0 °C. The inset shows the enlarged plot of the dashed area. Arrows correspond to the positions of pK_a values.

The potentiometric pH titration curve is shown in Figure 1 and the inset shows the enlarged plot of the dashed area. Two pK_a values are obtained at the relatively flat regions in the titration curve for three pH-sensitive groups. The two α amino groups of glutamic acid in 12-G(NH_2)LG(NH_2)-12 show an identical apparent pK_a value, i.e., 7.0. The pK_a value of the α carboxyl group of lysine is 5.2. Compared with the pK_a values of the corresponding groups in individual glutamic acid and lysine (9.7 and 2.2), the introduction of two alkyl chains significantly decreases the pK_a of the amino groups while increases the pK_a of the carboxyl group. Similar phenomena have been reported in many amino acid-based surfactant systems,[26-28] and two possible reasons were proposed. On one hand, the attachment of hydrophobic alkyl chains reduces the hydration of the peptide sequence. On the other hand, the hydrophobic interaction among the attached alkyl chains promotes the self-assembly of peptide surfactants. The self-assembly reduces the ionization extent of the pH-sensitive groups in the peptide to weaken the unfavorable intermolecular electrostatic repulsion. Thus the introduction of alkyl chains increases the pK_a of the carboxyl group and decreases the pK_a of the amino groups.

According to the pK_a values, the corresponding compositions and net charges of 12-G(NH_2)LG(NH_2)-12 at different pHs are calculated and presented in Figure 2A and 2B (black line). The compositions include 2NH_3^+-COOH, 2NH_3^+-COO^- and 2NH_2-COO^- species. 12-G(NH_2)LG(NH_2)-12 carries two positive charges below pH 4.0 and one negative charge above pH 9.0. Between them, the net charge of 12-G(NH_2)LG(NH_2)-12 gradually changes from two positive charges to one negative charge as pH increases. The isoelectric point (IEP) of this surfactant is at 7.0, where the peptide surfactant carries no net electrical charge.

The real charge property of 12-G(NH_2)LG(NH_2)-12 in aqueous solution over the entire pH studied has also been examined by ζ-potential measurement with 0.20 mM 12-G(NH_2)LG(NH_2)-12, as shown in Figure 2B (blue line). The ζ-potential curve experiences the same transition trend as the calculated net charge values, from positive, zero, and then to negative as pH increases.

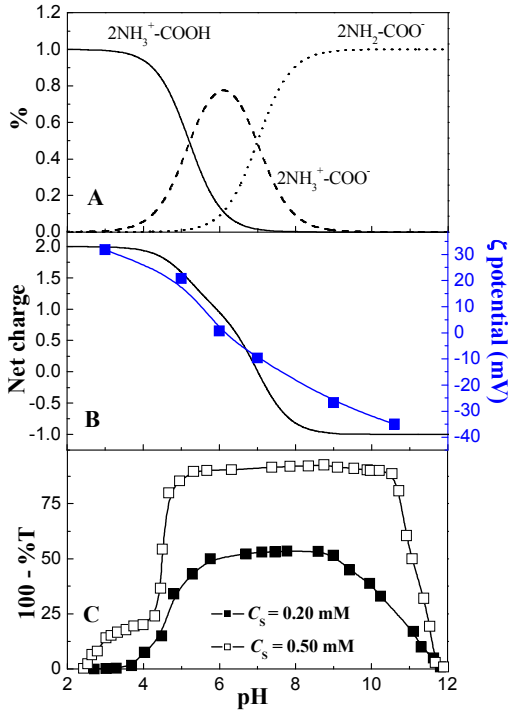

Fig. 2 Variations of (A) distributions of the 12-G(NH_2)LG(NH_2)-12 compositions, (B) calculated net charge values (black line) and ζ potential values (blue line) of 0.20 mM 12-G(NH_2)LG(NH_2)-12, and (C) turbidities of 0.20 and 0.50 mM 12-G(NH_2)LG(NH_2)-12 against the pH value at 25.0 °C.

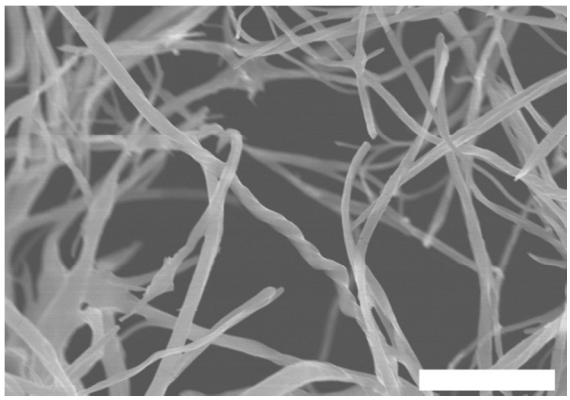

Fig. 3 SEM image of precipitates in 0.20 mM 12-G(NH_2)LG(NH_2)-12 solution at pH 7.0. Scale bar = 5 μm.

Phase behavior with pH

As described above, 12-G(NH_2)LG(NH_2)-12 shows different charge properties and charge amounts as pH changes. So pH change may trigger the phase behavior of 12-G(NH_2)LG(NH_2)-12 in aqueous solution.

To monitor the phase behavior of 12-G(NH_2)LG(NH_2)-12 at different pHs, the turbidity method was used, from which it can be determined whether the aggregate transition takes place and where transition points are located. The turbidity curves of 0.20 and 0.50 mM 12-G(NH_2)LG(NH_2)-12 solutions are plotted against pH in Figure 2C. Both the turbidity curves exhibit similar changing tendency upon increasing pH. At low pH or high pH, the turbidity is small and the solutions are optically transparent. The surfactant aggregates in these regions are well soluble in water. In these regions, the aggregates are highly positively or negatively charged as shown by the ζ-potential value. The positive charges are from the two protonated amino groups at the peptide sequence and the negative charge is from the carboxylate group in 12-G(NH_2)LG(NH_2)-12. The strong electrostatic repulsion among the charges keeps the aggregates soluble. When pH is beyond 4, the turbidity starts to sharply increase and the ζ-potential value becomes smaller. The 12-G(NH_2)LG(NH_2)-12 solution turns into a semitransparent bluish appearance This means that the pH increase reduces the net positive charge amount of 12-G(NH_2)LG(NH_2)-12, weakens intermolecular electrostatic repulsion, and thus significantly promotes the aggregation of 12-G(NH_2)LG(NH_2)-12. Beyond pH 5, the turbidity nearly does not change anymore in a wide pH range, and precipitation takes place. When pH increases up to 9 (0.20 mM 12-G(NH_2)LG(NH_2)-12) or 11 (0.50 mM 12-G(NH_2)LG(NH_2)-12), the precipitates start to redissolve, and the solution turns into bluish again accompanied by a marked decrease in turbidity. The large aggregates are formed by weakly negatively charged 12-G(NH_2)LG(NH_2)-12. In the precipitation range, both the ζ potential and the calculated charge amount are very close to zero. So precipitation takes place when 12-G(NH_2)LG(NH_2)-12 is close to charge neutralization. In addition, the higher concentration of 12-G(NH_2)LG(NH_2)-12 presents a much wider precipitation region, which means that increasing the concentration significantly promotes the aggregation by increasing the hydrophobic interaction among the alkyl chains. The SEM image (Figure 3) shows the precipitates consist of twisted and untwisted fibrils with hundreds of nanometers in diameter and tens of micrometers in length. The one-dimensional growth of the fibrils is probably driven by a combination of hydrophobic interaction among the alkyl chains and the hydrogen bond between the peptide sequences in 12-G(NH_2)LG(NH_2)-12, which will be further discussed in the later text.

Considering that the phase separation limits practical applications of 12-G(NH_2)LG(NH_2)-12 as a surfactant, the following investigations are carried out at pHs 3.0 and 11.0, where the 12-G(NH_2)LG(NH_2)-12 aggregates are all soluble. .

Aggregate transitions with concentration at pHs 3.0 and 11.0

At first, surface tension and ITC measurements were introduced to investigate the air/water interfacial and bulk properties of 12-G(NH_2)LG(NH_2)-12 in the basic and acidic solutions. The surface tension (γ) and observed enthalpy change (ΔH_{obs}) at pHs 3.0 and 11.0 are plotted against the final 12-G(NH_2)LG(NH_2)-12 concentration (C_s) in Figure 4. The surface tension measurements were made by titrating water into the 12-G(NH_2)LG(NH_2)-12 solution, while the ITC measurements were done by titrating the 12-G(NH_2)LG(NH_2)-12 solution into water. The initial concentrations of 12-G(NH_2)LG(NH_2)-12 titrated into water in the ITC experiments are 0.40 mM at pH 3.0, and 0.50 and 1.5 mM at pH 11.0.

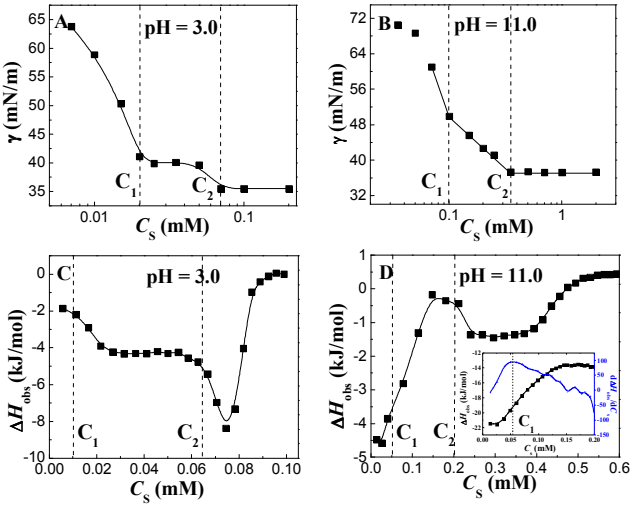

Fig. 4 Variations of (A and B) surface tension (γ) and (C and D) the observed enthalpy change (ΔH_{obs}) as a function of the 12-G(NH_2)LG(NH_2)-12 concentration at pHs 3.0 and 11.0. The dashed lines are referred to the two transition points C_1 and C_2. To illustrate how to determine the transition points, a representative differential curve (blue line) is shown with the ΔH_{obs} curve for titrating 0.50 M 12-G(NH_2)LG(NH_2)-12 into water at pH 11.0 in the inset of D.

All the surface tension and ITC curves strongly depend on the 12-G(NH_2)LG(NH_2)-12 concentration. The complicated changing patterns are totally different from those for normal single-component surfactants. Single-component surfactants normally only have one transition point in surface tension and ITC curves, which corresponds to critical micelle concentration (CMC). However in the present system, two obvious transition points exist in the γ-C_s curves at both pHs upon increasing the surfactant concentration. The ITC curves are even more complicated. By the

Cite this: DOI: 10.1039/c0xx00000x

www.rsc.org/xxxxxx

ARTICLE TYPE

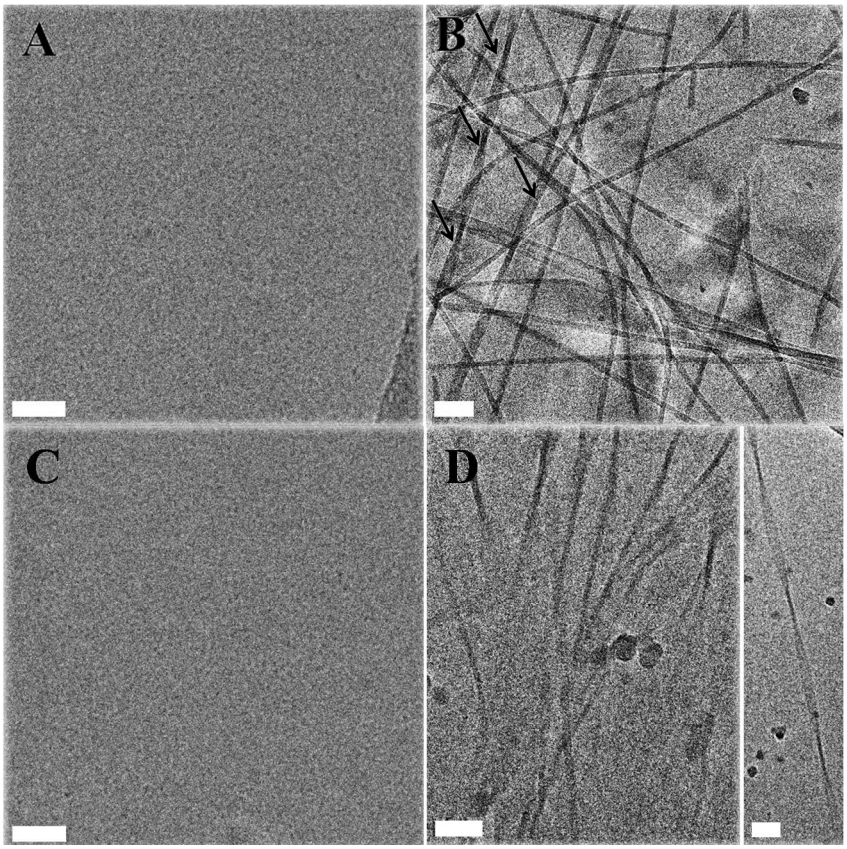

Fig. 5 Cryo-TEM images for the 12-G(NH_2)LG(NH_2)-12 solutions of different concentrations and pHs. (A) 0.04 mM, pH 3.0; (B) 0.20 mM, pH 3.0; (C) 0.20 mM, pH 11.0; and (D) 1.00 mM, pH 11.0. Scale bar = 50 nm.

aid of differentiating the ITC curves, two transition points can be determined too. The two transition points derived from the surface tension and ITC curves are very close with each other, as shown in Figure 4. The results suggest that 12-G(NH_2)LG(NH_2)-12 at both pHs experiences three kinds of aggregation modes at interface and in bulk solution simultaneously.

In order to understand the variations of the surface tension and ITC curves, the 12-G(NH_2)LG(NH_2)-12 solutions located between C_1 and C_2, and above C_2 are observed by Cryo-TEM. The representative Cryo-TEM images of the 12-G(NH_2)LG(NH_2)-12 aggregates are illustrated in Figure 5. The Cryo-TEM images indicate that 12-G(NH_2)LG(NH_2)-12 at pHs 3.0 and 11.0 experiences similar aggregate transitions. Between C_1 and C_2, 12-G(NH_2)LG(NH_2)-12 forms small spherical micelles of 2~3 nm at both pHs (Figure 5A, 5C). Above C_2, the small micelles transfer into stiff fibers of ~30 nm in width and several micrometers in length at pH 3.0 (Figure 5B), and transfer into twisted ribbons at pH 11.0 (Figure 5D). In Figure 5B, some fibers tend to further aggregate into bundles of twisted structure.

Then we return to the surface tension and ITC curves. Below C_1, the surface tension value is large and rapidly decreases with increasing the 12-G(NH_2)LG(NH_2)-12 concentration. This is one of the typical features of surfactants below CMC. The 12-G(NH_2)LG(NH_2)-12 molecules in this stage exist as solvated monomers in thermodynamic equilibrium with those at air/water interface. Between C_1 and C_2, the surface tension at pH 3.0 reaches a plateau (~ 40 mN/m), while the surface tension at pH 11.0 continues to decrease but the decreasing rate is much lower than that below C_1. The unchanged and lower decreasing surface tension values indicate that 12-G(NH_2)LG(NH_2)-12 at air/water interface has reached or approached saturation and the added 12-G(NH_2)LG(NH_2)-12 starts to associate into aggregates in bulk solution above C_1. According to the above Cryo-TEM results, the formed aggregates are small micelles. Thus the first transition point C_1 corresponds to the CMC. In the micellization process, the ITC curves display an exothermic ΔH_{obs} value, and the ΔH_{obs} value at pH 3.0 is less exothermic than at pH 11.0. With increasing the 12-G(NH_2)LG(NH_2)-12 concentration beyond C_1, the ITC curve at pH 3.0 significantly changes to more exothermic ΔH_{obs} values, while the ITC curve at pH 11.0 becomes less exothermic. After that, both the exothermic ΔH_{obs} values remain almost unchanged until C_2. The ITC curves in this process are

approximately sigmoidal in shape at pHs 3.0 and 11.0, showing the feature of surfactant micellization. The apparent enthalpy change of micellization (ΔH_{mic}) can be derived from the difference between the two linear segments of the plots extrapolated to the CMC.[6] The ΔH_{mic} value at pH 3.0 is -2.4 KJ/mol and the ΔH_{mic} value at pH 11.0 is 4.3 KJ/mol. Moreover the ITC curve in this stage at pH 3.0 is like those of ionic surfactants, while the ITC curve in this stage at pH 11.0 is more like those for nonionic surfactants.

Above C_2, the surface tension decreases to the second plateau, ~35 mN/m at pH 3.0 and ~37 mN/m at pH 11.0, and the surface tension does not decrease anymore. This indicates that the 12-G(NH_2)LG(NH_2)-12 molecules beyond C_2 are packed more tightly at air/water interface than at lower concentration, and the surface activity of the 2-G(NH_2)LG(NH_2)-12 molecules at pHs 3.0 and 11.0 are very similar. Correspondingly, the ITC curves experience the following changes: falling down to more exothermic ΔH_{obs}, arising back to zero and remaining unchanged. Herein, the 2-G(NH_2)LG(NH_2)-12 forms fibers at pH 3.0 and twisted ribbons at pH 11.0 as shown in the Cryo-TEM images,. The exothermic peak of ΔH_{obs} is attributed to the aggregate transition from small spherical micelles to the fibers or twisted ribbons, and the larger exothermic enthalpy indicates that the transition is driven by the significantly enhanced hydrophobic interaction may be accompanied with the decreasing of ionization degree of the charged groups in the peptide spacer. Therefore, the second transition points C_2 is the critical concentration for this aggregate transition. Two transition points were also derived from the surface tension curves in several amino acid surfactants, such as sodium *N*-(11-acrylamidoundecanoyl)-L-serinate, L-asparaginate, and L-glutaminate aqueous solutions, and the second transition corresponds to the formation of planar bilayer aggregates or closed veisicles.[29]

Beside, the two critical concentrations of 12-G(NH_2)LG(NH_2)-12 at pH 3.0 are smaller than those at pH 11.0, suggesting that the self-assembling ability of 12-G(NH_2)LG(NH_2)-12 is stronger in the acidic solution. As known, the peptide-based surfactant aggregation is mainly controlled by a combination of electrostatic interaction among ionic headgroups, hydrogen bond between the peptide sequence and hydrophobic association among alkyl chains. As discussed above, each 12-G(NH_2)LG(NH_2)-12 molecule carries two positive charges at pH 3.0 and one negative charge at pH 11.0. The electrostatic repulsion among the ionic headgroups of 12-G(NH_2)LG(NH_2)-12 at pH 3.0 should be stronger than that at pH 11.0, which is unfavorable to the surfactant aggregation. Considering the same alkyl chains at both pHs, the stronger aggregation ability of 12-G(NH_2)LG(NH_2)-12 at pH 3.0 is probably attributed to stronger intermolecular hydrogen bonds between the peptide sequences. As we discussed previously,[6] the two charges in the middle of the peptide moiety enhance electrostatic repulsion and disorder the hydrogen bonding which induces a random coil secondary structure. On the contrary, their separate locations at two terminals of the peptide facilitate the formation of hydrogen bonds and lead to the formation of ordered β-sheet secondary structure.

In the following text, in order to further understand the pH effects on the hydrogen bonds, CD spectra is used to study the secondary structure of the peptide spacer of 12-G(NH_2)LG(NH_2)-12.

Secondary structure of peptide spacer at pHs 3.0 and 11.0

The CD spectra of the 12-G(NH_2)LG(NH_2)-12 solution beyond C_2 at pHs 3.0 and 11.0 are shown in Figure 6. The 12-G(NH_2)LG(NH_2)-12 concentration at pH 3.0 is 0.20 mM at which well-defined fibers are formed, and the 12-G(NH_2)LG(NH_2)-12 concentration at pH 11.0 is 1.0 mM at which twisted ribbons are formed.

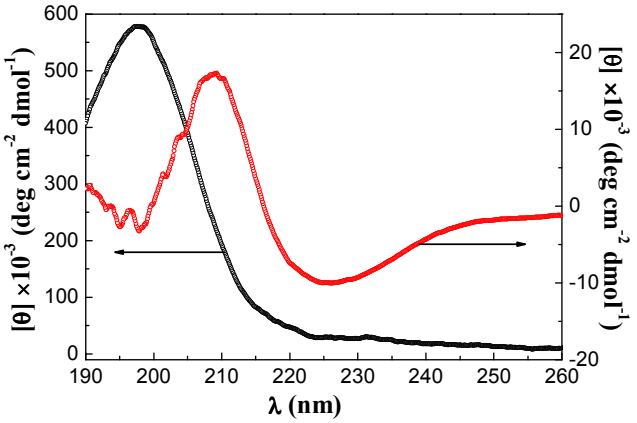

Fig. 6 CD spectra of the 12-G(NH_2)LG(NH_2)-12 solutions at 0.20 mM concentration and pH 3.0 (black line) and at 1.0 mM concentration and pH 11.0 (red line).

Previous works[30,31] on peptide-based surfactants have shown that the high-aspect-ratio assembly of entities is inherently related to β-sheet structure accompanied by a β-sheet signal in CD. The typical CD spectrum of the peptide β-sheet conformation has a maximum at 195 nm and a minimum at 216 nm.[32] Here, the CD spectrum at pH 11.0 with a maximum at ~213 nm and a minimum at ~225 nm (red line) is predominantly attributed to the β-sheet structure. These signals are red-shifted relative to those in typical β-sheet structures. This phenomenon has been demonstrated to be caused by a twisted or disordered structure, which is resulted from weak hydrogen bonds.[33] However, the CD spectrum at pH 3.0 is completely different from that at pH 11.0. The positive peak around ~196 nm is very close to that of a β-sheet structure with a very profound value but the negative signal is absent. Similar phenomenon was reported earlier in peptide-based surfactant systems where a chiral supermolecular structure-helical fiber was formed.[21] The long range order of a chiral supermolecular structure was assumed to be able to amplify the signals. In the present result at pH 3.0, two or more fibers aggregate into bundles of twisted structure that could account for the deviation of the corresponding CD spectrum from the β-sheet structure.

Possible molecular packing

As mentioned above, Abe's group[24] reported the aqueous binary phase diagram of the gemini peptide surfactant 12-GLG-12 which carries three negatively charged carboxylates. Due to the strong electrostatic repulsion between the three negative charges, the surfactant molecules form micelles above the critical micelle concentration and the surfactant exists as micelles even if the concentration is up to 32 wt%. Beyond the micellar region, the surfactant forms micellar cubic phase, hexagonal liquid crystal

and lamellar liquid crystal with the increase of concentration. However, although the molecular structure of 12-G(NH2)LG(NH2)-12 is very similar to that of 12-GLG-12, the aggregation behavior is much more complicated at low concentration. Figure 7 shows a schematic representation for the aggregates formed by 12-G(NH2)LG(NH2)-12 at pHs 3.0 and 11.0. The variation in aggregate morphologies of 12-G(NH_2)LG(NH_2)-12 at different pHs should be caused by the different manners of the intermolecular interactions in the self-assemblies. The two alkyl chains in 12-G(NH2)LG(NH2)-12 provide a hydrophobic synergetic force in self-assembly process to construct a hydrophobic core. The hydrogen bonds between the peptide moieties are highly aligned and directed. Moreover the locations of the charges in the peptide affect the direction and strength of the hydrogen bonds. Meanwhile the hydrophobic interaction among the alkyl chains is directed by the hydrogen bonds. The electrostatic repulsion of the peptide moieties can also change the aggregate curvature of the 12-G(NH2)LG(NH2)-12 assemblies. All these intermolecular interactions influence each other and cooperatively control the final self-assembling structures.

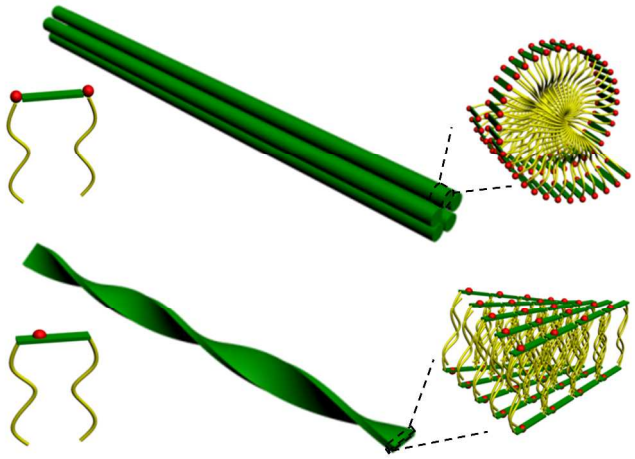

Fig. 7 Schematic representation of a nanofiber at pH 3.0 (top) and a twisted ribbon at pH 11.0 (bottom) formed by 12-G(NH2)LG(NH2)-12.

As shown in the top of Figure 7, which represents the situation of the 12-G(NH2)LG(NH2)-12 aggregates at pH 3.0, two positively charged amino groups are situated at the two ends of the peptide spacer and the carboxyl group located in the middle is uncharged. The electrostatic repulsion between the positive amino groups of different molecules does not obviously affect the hydrogen bonds between other groups in the spacer. The carboxyl group and the amide groups in the middle of the peptide spacer prefer to form ordered intermolecular hydrogen bonds. Thus the peptide sequence takes a *β*-sheet structure in which the peptide spacer of each 12-G(NH2)LG(NH2)-12 molecule is aligned side by side and the hydrophobic interaction among the alkyl chains draws the chains close to each other. Meanwhile, the strong electrostatic repulsion between the positive charges in the neighboring peptide headgroups leads to a highly curved and slightly twisted structure in the self-assemblies. Therefore the 12-G(NH2)LG(NH2)-12 molecules form a cylindrical structure with the hydrophilic peptide moieties exposed to water and the hydrophobic chains crimped inward. However, as shown in the bottom of Figure 7, the 12-G(NH2)LG(NH2)-12 aggregates at pH 11.0 are different. The carboxyl group and the two amino groups are all deprotonated, and then the carboxyl group is negatively charged, while the amino groups are neutral. There is only one charged group in the middle of the peptide spacer. On one hand, this weakens the intermolecular electrostatic repulsion of the peptide spacers. On the other hand, the location of the charged carboxyl group in the middle of the peptide spacer disfavors the hydrogen bonding of the nearby amide groups, causing the peptide to adopt a more twisted *β*-sheet structure. Therefore the 12-G(NH2)LG(NH2)-12 molecules form a lamellar structure and result in the twisted ribbons. The twisting of the *β*-sheets leads to a small rotation between the adjacent 12-G(NH2)LG(NH2)-12 molecules one by one along the long axis of the ribbons. This manner of molecular packing may balance the electrostatic repulsion of the negative charges and ensure the formation of the hydrogen bonds of the peptide spacer as much as possible, while keep the hydrophobic chains close to each other.

Conclusions

The present work has studied the effects of pH and concentration on the aggregation behavior of a gemini surfactant taking glutamic acid-lysine-glutamic acid peptide as a spacer. The results show that the gemini surfactant 12-G(NH_2)LG(NH_2)-12 can self-assemble into fiber-like precipitates over the pH range where 12-G(NH_2)LG(NH_2)-12 carries almost no net charges, and the amount and range of precipitates increase with increasing concentration. The ordered precipitates result from hydrophobic interaction among alkyl chains and directional hydrogen bonds of the peptide sequences. 12-G(NH_2)LG(NH_2)-12 forms soluble aggregates at pHs 3.0 and 11.0 because each 12-G(NH2)LG(NH2)-12 carries two positively charged amino groups at the two ends of the peptide spacer at pH 3.0, while each 12-G(NH2)LG(NH2)-12 carries one negatively charged carboxyl group on the middle of the peptide spacer at pH 11.0. It is demonstrated that 12-G(NH2)LG(NH2)-12 has two transition points with increasing concentration at these two pHs: critical micelle concentration and the critical transition concentration from small micelles to fibers or twisted ribbons. The concentration induced aggregate transition from micelles to fibers or twisted ribbons is attributed to the enhanced hydrophobic interaction among the alkyl chains as well as the β-sheet structure formation controlled by the hydrogen bonds between the peptide spacers. The different assemblies of 12-G(NH_2)LG(NH_2)-12 at different pHs arise from the different extents of twist and disorder in the β-sheet structure, being determined by many intermolecular interactions. The two alkyl chains provide a synergetic hydrophobic force to form a hydrophobic core, and the hydrophobic interaction among the alkyl chains is directed by the hydrogen bonds. The hydrogen bonds between the peptide moieties are aligned and directed. The location of the charges in the peptide spacer affects the direction and strength of the hydrogen bonds, and the electrostatic repulsion of the charges gradually adjusts the aggregate curvature of the assemblies. In final, the balance of these interactions determines the self-assembling structures of the peptide gemini surfactant. This observation highlights the significance of the number and

location of charges in the self-assembly process and the resulting nanostructures of a gemini surfactant with a peptide spacer. This work presents additional understanding in manipulating the aggregation behavior of a peptide-based surfactant and may show some guidance in developing peptide gemini surfactants applied in industry and daily life.

Acknowledgments

We are grateful for financial supports from National Natural Science Foundation of China (Grants 21025313, 21321063).

Notes and references

Key Laboratory of Colloid and Interface Science, Beijing National Laboratory for Molecular Sciences (BNLMS), Institute of Chemistry, Chinese Academy of Sciences, Beijing, China. Fax: 86-10-82615802; Tel: 86-10-82615802; E-mail: yilinwang@iccas.ac.cn.

† Electronic Supplementary Information (ESI) available: MS spectra, analytical HPLC chromatograms and ^{1}H NMR spectra of 12-G(NH_2)LG(NH_2)-12. See DOI: 10.1039/b000000x/

1 M. C. Morán, A. Pinazo, L. Pérez, P. Clapés, M. Angelet, M. T. García, M. P. Vinardell and M. R. Infante, *Green Chem.*, 2004, **6**, 233–240.
2 X. B. Zhao, F. Pan, H. Xu, M. Yaseen, H. H. Shan, C. A. E. Hauser, S. G. Zhang and J. R. Lu, *Chem. Soc. Rev.*, 2010, **39**, 3480–3498.
3 L. Pérez, A. Pinazo, R. Pons and M. Infante, *Adv. Colloid Interface Sci.*, 2014, **205**, 134–155.
4 R. N. Mitra, A. Shome, P. Paul and P. K. Das, *Org. Biomol. Chem.*, 2009, **7**, 94–102.
5 K. Arima, A. Kakinuma and G. Tamura, *Biochem. Biophys. Res. Commun.*, 1968, **31**, 488–494.
6 M. L. Deng, D. F. Yu, Y. B. Hou and Y. L. Wang, *J. Phys. Chem. B*, 2009, **113**, 8539–8544.
7 D. Khatua and J. Dey, *J. Phys. Chem. B*, 2007, **111**, 124–130.
8 U. Khoe, Y. L. Yang and S. G. Zhang, *Langmuir*, 2009, **25**, 4111–4114.
9 H. Tsutsumi and H. Mihara, *Amino Acids, Pept. Proteins*, 2013, **38**, 122–150.
10 D. W. P. M. Löwik and J. C. M. V. Hest, *Chem, Soc. Rev.*, 2004, **33**, 234–245.
11 S. Y. Qin, S. S. Xu, R. X. Zhuo and X. Z. Zhang, *Langmuir*, 2012, **28**, 2083–2090.
12 C. Q. He, Y. C. Han, Y. X. Fan, M. L. Deng and Y. L. Wang, *Langmuir*, 2012, **28**, 3391–3396.
13 Y. T. Fu, B. Z. Li, Z. B. Huang, Y. Li and Y. G. Yang, *Langmuir*, 2013, **29**, 6013–6017.
14 Y. Y. Lin, Y. Qiao, P. F. Tang, Z. B. Li and J. B. Huang, *Soft Matter*, 2011, **7**, 2762–2769.
15 J. D. Hartgerink, E. Beniash and S. I. Stupp, *Science*, 2001, **294**, 1684–1688.
16 R. M. Levine, C. M. Scottb and E. Kokkoli, *Soft Matter*, 2013, **9**, 985–1004.
17 M. Sardan, M. Kilinc, R. Genc, A. B. Tekinay and M. O. Guler, *Faraday Discuss.*, 2013, **166**, 269–283.
18 X. Zhao, Y. Nagai, P. J. Reeves, P. Kiley, H. G. Khorana and S. Zhang, *Proc. Natl. Acad. Sci. U. S. A.*, 2006, **103**, 17707–17712.
19 T. Shimada, Y. Tamura, M. Tirrell and K. Kuroda, *Chem. Lett.*, 2012, **41**, 95–97.
20 M. Zhou, A. M. Smith, A. K. Das, N. W. Hodson, R. F. Collins, R. V. Ulijn and G. E. Gough, *Biomaterials*, 2009, **30**, 2523–2530.
21 D. W. P. M. Löwik, J. Garcia-Hartjes, J. T. Meijer and J. C. M. V. Hest, *Langmuir*, 2005, **21**, 524–526.
22 T. J. Moyer, H. G. Cui and S. I. Stupp, *J. Phys. Chem. B*, 2013, **117**, 4604–4610.
23 T. Gore, Y. Dori, Y. Talmon, M. Tirrell and H. Bianco-Peled, *Langmuir*, 2001, **17**, 5352–5360.
24 R. G. Shrestha, K. Nomura, M. Yamamoto, Y. Yamawaki, Y. Tamura, K. Sakai, K. Sakamoto, H. Sakai and M. Abe, *Langmuir*, 2012, **28**, 15472–15481.
25 Z. Hu, X. Tian, Y. Zhai, W. Xu, D. Zheng and F. Sun, *Protein Cell*, 2010, **1**, 48–58.
26 A. Colomer, A. Pinazo, M. T. García, M. Mitjans, M. P. Vinardell, M. R. Infante, V. Martínez and L. Pérez, *Langmuir*, 2012, **28**, 5900–5912.
27 M. Spelios and M. Savva, *FEBS J.*, 2008, **275**, 148–162.
28 A. Pinazo, L. Pérez, M. R. Infante and R. Pons, *Phys. Chem. Chem. Phys.*, 2004, **6**, 1475–1481.
29 S. Roy and J. Dey, *J. Colloid Interface Sci.*, 2007, **307**, 229–234.
30 E. T. Pashuck, H. G. Cui and S. I. Stupp, *J. Am. Chem. Soc.*, 2010, **132**, 6041–6046.
31 S. E. Paramonov, H. W. Jun and J. D. Hartgerink, *J. Am. Chem. Soc.*, 2006, **128**, 7291–7298.
32 R. W. Woody, *Methods Enzymol.*, 1995, **246**, 34–71.
33 M. C. Manning, M. Illangasekare and R. W. Woody, *Biophys. Chem.*, 1988, **31**, 77–86.

TOC Graphic

Aggregation behavior of a gemini surfactant with a tripeptide spacer

Meina Wang, Yuchun Han, Fulin Qiao and Yilin Wang*

Key Laboratory of Colloid and Interface Science, Beijing National Laboratory for Molecular Sciences (BNLMS), Institute of Chemistry, Chinese Academy of Sciences, Beijing 100190, People's Republic of China.

FAX: +86 010 82615807, E-mail: yilinwang@iccas.ac.cn

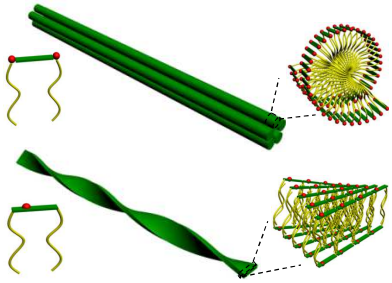

A gemini surfactant with a tripeptide spacer shows strong pH-dependent and concentration-dependent aggregation behavior.